

# Discriminative Link Prediction using Local Links, Node Features and Community Structure

Abir De  
IIT Kharagpur, India  
abir.de@cse.iitkgp.ernet.in

Niloy Ganguly  
IIT Kharagpur, India  
niloy@cse.iitkgp.ernet.in

Soumen Chakrabarti  
IIT Bombay, India  
soumen@cse.iitb.ac.in

**Abstract**—A link prediction (LP) algorithm is given a graph, and has to rank, for each node, other nodes that are candidates for new linkage. LP is strongly motivated by social search and recommendation applications. LP techniques often focus on global properties (graph conductance, hitting or commute times, Katz score) or local properties (Adamic-Adar and many variations, or node feature vectors), but rarely combine these signals. Furthermore, neither of these extremes exploit link densities at the intermediate level of communities. In this paper we describe a discriminative LP algorithm that exploits two new signals. First, a co-clustering algorithm provides community level link density estimates, which are used to qualify observed links with a surprise value. Second, links in the immediate neighborhood of the link to be predicted are not interpreted at face value, but through a local model of node feature similarities. These signals are combined into a discriminative link predictor. We evaluate the new predictor using five diverse data sets that are standard in the literature. We report on significant accuracy boosts compared to standard LP methods (including Adamic-Adar and random walk). Apart from the new predictor, another contribution is a rigorous protocol for benchmarking and reporting LP algorithms, which reveals the regions of strengths and weaknesses of all the predictors studied here, and establishes the new proposal as the most robust.

## 1. INTRODUCTION

The link prediction (LP) problem [16] is to predict future relationships from a given snapshot of a social network. E.g., one may wish to predict that a user will like a movie or book, or that two researchers will coauthor a paper, a user will endorse another on LinkedIn, or two users will become “friends” on Facebook. Apart from the obvious recommendation motive, LP can be useful in social search, such as Facebook Graph Search<sup>1</sup>, as well as ranking goods or services based on not only real friends’ recommendations but also that of imputed social links.

Driven by these strong motivations, LP has been intensively researched in recent years; Lu and Zhou [19] provide a comprehensive survey. As we shall describe in Section 2, in trying to predict if nodes  $u, v$  in a social network are likely to be(come) related, LP approaches predominantly exploit three kinds of signals:

- When nodes have associated feature vectors (user demography, movie genre), node-to-node similarity may help predict linkage.
- Local linkage information, such as the existence of many common neighbors, may hint at linkage. The well-known Adamic-Adar (AA) [1] predictor and variants use such information.

- Non-local effects of links, such as effective conductance, hitting time, commute time [7], or their heuristic approximations are often used as predictors. The Katz score [12] is a prominent example. The random walk paradigm has also been combined [2] with edge features for enhanced accuracy.

Recently, stochastic block models [8], factor models and low-rank matrix factorization [15] have been used to “explain” a dyadic relation using a frugal generative model. These have rich connections to coding and compression. Co-clustering [6] and cross-association [4] are related approaches. Co-clustering exposes rich block structure in a dyadic<sup>2</sup> relation. E.g., in a user-movie matrix, it can reveal that some users like a wide variety of movies whereas others are more picky, or that some classic movies are liked by all clusters of people.

Although co-clustering provides a *regional* community density signal, it is derived of global linkage considerations, and is arguably more meaningful than global, unbounded random walks. However, exploiting the signal from co-clustering is non-obvious. The generative model implicit in co-clustering is that edges in each dyadic block are sampled iid from a Bernoulli distribution with a parameter corresponding to the empirical edge density in the block. While the choices of blocks and their edge densities offer optimal global compression, they cannot predict presence or absence of *individual links* without incorporating node features and local linkage information.

Our key contribution (Section 4) is a new two-level learning algorithm for LP. At the lower level, we learn a local model for similarity of nodes across edges (and non-edges). This is combined, using a support vector machine, with an entirely new non-local signal: the output of co-clustering [6], suitably tuned into feature values.

To the best of our knowledge, this is the first work that brings all three sources of information (node features, immediate neighborhood, “regional” community structure) together in a principled way. Another contribution (Section 3) is a rigorous evaluation protocol for LP algorithms, using a new binning strategy for nodes based on their local link structure. The new protocol reveals the strengths and weaknesses of LP algorithms across a range of operating conditions.

On five diverse and public data sets (NetFlix, MovieLens, CiteSeer, Cora, WebKb) that are standard in the LP community, our algorithm offers (Section 5) substantial accuracy gains beyond strong baselines. Our main experimental observations

<sup>1</sup><https://www.facebook.com/about/graphsearch>

<sup>2</sup>Can be extended to larger arity.

are:

- The local similarity model on edges beats baselines in some regions of the problem space, but is not overall significantly better.
- The additional signal from communities, found through co-clustering, is strong and helpful.
- A global discriminative learning technique using the above signals convincingly beats baselines.

## 2. RELATED WORK

LP has been studied in different guises for many years, and formalized, e.g., by Liben-Nowell and Kleinberg [16]. Lu and Zhou [19] have written a comprehensive survey.

### 2.1. Local similarity

If each node  $u$  is associated with a feature vector  $\theta_u$ , these can be used to define edge feature vectors  $f(u, v) = f(\theta_u, \theta_v)$ , which can then be involved in an edge prediction through logistic regression (i.e.,  $\Pr(\text{edge}|u, v) = \frac{1}{1+e^{-\nu \cdot f(u, v)}}$ ), or a SVM (predict an edge if  $\nu \cdot f(u, v) > 0$ ). Obviously, this class of models miss existing neighborhood information.

To decide if nodes  $u$  and  $v$  may get linked, one strong signal is the number of common neighbors they already share. Adamic and Adar (AA) [1] refined this by a weighted counting: common neighbors who have many other neighbors are dialed down in importance:

$$\text{sim}_{i,j}^{\text{AA}} = \sum_{k \in \Gamma(i) \cap \Gamma(j)} \frac{1}{\log d(k)}, \quad (1)$$

where  $d(k)$  is the degree of common neighbor  $k$ .

The resource allocation (RA) predictor is a slight variation which replaces  $\log d(k)$  with  $d(k)$  in (1). The AA and RA predictors both penalize the contribution of high-degree common neighbors. The difference between them is insignificant if  $d(k)$  is small. However they differ for large  $d(k)$ . RA punishes the high-degree common neighbors more heavily than AA. Among ten local similarity measures, Lu and Zhou found [19, Table 1, page 9] RA to be the most competitive, and AA was close.

### 2.2. Random walks and conductance

AA, RA, etc. are specific examples of three general principles that determine large graph proximity between nodes  $u$  and  $v$ :

- Short path(s) from  $u$  to  $v$ .
- Many parallel paths from  $u$  to  $v$ .
- Few distractions (high degree nodes) on the path(s).

Elegant formal definitions of proximity, that capture all of the above, can be defined by modeling the graph  $(V, E)$  ( $|V| = N, |E| = M$ ) as a resistive network and measuring effective conductance, or equivalently [7], modeling random walks [14], [22], [21] on the graph and measuring properties of the walk. Many link predictors are based on such proximity estimates. The earliest, from 1953 [12], defines

$$\text{sim}_{\text{Katz}}(u, v) = \beta A_{uv} + \beta^2 (A^2)_{uv} + \dots = (\mathbb{I} - \beta A)^{-1} - \mathbb{I}, \quad (2)$$

where  $A$  is the (symmetric) adjacency matrix and  $\beta < 1/\lambda_1$ , the reciprocal of the largest eigenvalue of  $A$ . This is effectively a length-weighted count of the number of paths between  $u$  and  $v$ . Lu and Zhou [19] describe several other related variants. In their experiments, the best-performing definition were local [22] and cumulative (called “superposed” by Lu and Zhou) random walks (LRW and CRW), described next.

Suppose  $q_u$  is the steady state visit probability of node  $u$  (degree divided by twice the number of edges in case of undirected graphs). Let  $\pi_u(0)$  be the impulse distribution at  $u$ , i.e.,  $\pi_u(0)[u] = 1$  and  $\pi_u(0)[v] = 0$  for  $v \neq u$ . Define  $\phi_u(t+1) = C^t \pi_u(t)$ , where  $C$  is the  $N \times N$  row-stochastic edge conductance (or transition probability) matrix. Then

$$\text{sim}_{uv}^{\text{LRW}}(t) = q_u \pi_u(t)[v] + q_v \pi_v(t)[u]. \quad (3)$$

For large  $t$ , the two rhs terms become equal, and LRW similarity is simply twice the “flow” of random surfers on the edge  $\{u, v\}$ . Lu and Zhou claimed [19, Table 3, page 16] that LRW is competitive, but the following cumulative random walk (CRW) is sometimes more accurate.

$$\text{sim}_{u,v}^{\text{CRW}}(t) = \sum_{\tau=1}^t \text{sim}_{u,v}^{\text{LRW}}(\tau). \quad (4)$$

CRW does not converge with increasing  $t$ , so  $t$  is chosen by validation against held-out data.

Although some of these approaches may feel ad-hoc, they work well in practice; Sarkar *et al.* [20] have given theoretical justification as to why this may be the case.

### 2.3. Probabilistic generative models

One of the two recent approaches that blend node features with linkage information is by Ho *et al.* [8], although it is pitched not as a link predictor, but as an algorithm to cluster hyperlinked documents into a Wikipedia-like hierarchy. (Documents directly correspond to social network nodes with local features.) The output is a tree of latent topic nodes, with each document associated with a leaf topic. The algorithm seeks to cluster similar documents into the same or nearby topic nodes, and reward topic trees with dense linkages between documents belonging to small topic subtrees rather than span across far-away topic nodes. The model associates a parameter  $\phi(t) \in (0, 1)$  with each topic node  $t$ . If documents  $u, v$  are attached to topic nodes  $t(u), t(v)$ , then the probability of a link between  $u, v$  is estimated as  $\phi(\text{LCA}(t(u), t(v)))$ , where LCA is least common ancestor. These probabilities can then be used to rank proposed links.

### 2.4. Supervised random walk (SRW)

The other approach to blend node features with graph structure is supervised and discriminative [2], and based on personalized PageRank [10]. Recall that  $f(u, v)$  is an edge feature vector. The raw edge weight is defined as  $a(u, v) = a(w \cdot f(u, v))$  for a suitable monotone function  $a(\cdot) > 0$ . The probability of a random surfer walking from  $u$  to  $v$  is set to

$$\Pr(u \rightarrow v) \stackrel{\text{def}}{=} C(u \rightarrow v) = C[v, u] = \frac{a(u, v)}{\sum_{v'} a(u, v')}.$$

where  $C \in \mathbb{R}^{N \times N}$  is called the *edge conductance matrix*. If we are trying to predict out-neighbors of source node  $s$ , we set up a teleport vector  $r_s$  defined as  $r_s[u] = 1$  if  $u = s$  and 0 otherwise, then find the personalized PageRank vector  $\text{PPV}_s$ , defined by the recurrence

$$\text{PPV}_s = \alpha C \text{PPV}_s + (1 - \alpha)r_s.$$

During training, for source node  $s$ , we are given some actual neighbors  $g$  and non-neighbors  $b$ , and we want to fit  $w$  so that  $\text{PPV}_s[g] > \text{PPV}_s[b]$ .

SRW is elegant in how it fits together edge features with visible graph structure, but the latter is exploited in much the same way as Katz or LRW. Specifically, it does not receive as input regional graph community information. Thus, SRW and our proposal exploit different sources of information. Unifying SRW with our proposal is left for future work.

### 2.5. Unsupervised random walk

Before SRW, Lichtenwalter *et al.* [17] introduced an unsupervised prediction method, PropFlow, which corresponds to the probability that a restricted random walk starting at  $v_i$  ends at  $v_j$  in some pre-specified  $l$  steps or fewer using link weights as transition probabilities. The restrictions are that the walk terminates upon reaching  $v_j$  or upon revisiting any other node. This produces a score  $s_{ij}$  which is used to predict new links. PropFlow is somewhat similar to rooted PageRank, but it is a more localized measure of propagation, and is insensitive to topological noise far from the source node. The salient features are: 1. the walk length is limited by  $l$  which is very small (4–5), so PropFlow is much faster than SRW, and 2. unlike PageRank, it does not need restarts and convergence but simply employs a modified breadth search method.

### 2.6. Co-clustering

Similar documents share similar terms, and vice versa. In general, clustering one dimension of a dyadic relation (represented as a binary matrix  $A$ , say) is synergistic with clustering the other. Dhillion *et al.* [6] proposed the first information-theoretic approach to group the rows and columns of  $A$  into separate row and column *groups* (also called *blocks*, assuming rows and columns of  $A$  have been suitably permuted to make groups occupy contiguous rows and columns) so as to best compress  $A$  using one link density parameter per (row group, column group) pair.

As we shall see, co-clustering and the group link densities can provide information of tremendous value to link prediction algorithms, of a form not available to AA, RA, LRW or CRW. In recommending movies to people, for instance, there are clusters of people that like most movies, and there are clusters of classic movies that most people like. Then there are other richer variations in block densities. Given a query edge in the LP setting, it seems natural to inform the LP algorithm with the density of the block containing the query edge.

However, the estimated block density is the result of a global optimization, and cannot directly predict one link. That requires combining the block density prior with local information (reviewed above). That is the subject of Section 4.

## 3. EVALUATION PROTOCOL

As described informally in Section 4.1, a LP algorithm applied to a graph snapshot is successful to the extent that *in future*, users accept high-ranking proposed links. In practice, this abstract view quickly gets murky, especially for graphs without edge creation timestamps, but also for those with timestamps. In this section we discuss the important issues guiding our evaluation protocol and measurements.

### 3.1. Labeling vs. ranking accuracy

Regarding the LP algorithm’s output as a binary prediction (edge present/absent) for each node pair, comparing with the true state of the edge, and counting up the fraction of correct decisions, is a bad idea, because of extreme skew in typical sparse social graphs: most potential edges are absent. The situation is similar to ranking in information retrieval (IR) [18], where, for each query, there are many fewer relevant documents than irrelevant ones. In LP, a separate ranking is produced for each node  $q$  from a set of nodes  $Q$ , which are therefore called *query nodes*.

Fix a  $q$  and consider the ranking of the other  $N - 1$  nodes. Some of these are indeed neighbors (or will end up becoming neighbors). Henceforth, we will call  $q$ ’s neighbors as *good* nodes  $G(q)$  and non-neighbors as *bad* nodes  $B(q)$ . Ideally, each good node should rank ahead of all bad nodes. Because the LP algorithm is generally imperfect, there will be exceptions. The area under the ROC curve (AUC) is widely used in data mining as a accuracy measure somewhat immune to class imbalance. It is closely related to the fraction of the  $|G(q)||B(q)|$  good-bad pairs that are in the correct order in LP’s ranking. However, for the same reasons as in IR ranking [18], AUC tends to be large and undiscerning for almost any reasonable LP algorithm. Therefore, we adapt standard ranking measure mean average precision (MAP).

At each node, given a score from the LP algorithm on all other nodes as potential neighbors, and the “secret” knowledge of who is or isn’t a neighbor, we compute the following performance metrics.

*3.1.1. Precision and recall:* These are defined as

$$\text{Precision}(k) = \frac{1}{|Q|} \sum_{q \in Q} P_q(k) \quad (5)$$

$$\text{and } \text{Recall}(k) = \frac{1}{|Q|} \sum_{q \in Q} R_q(k), \quad (6)$$

where  $|Q|$  is the number of queries,  $P_q(k)$  is Precision@ $k$  for query  $q$ , and  $R_q(k)$  is Recall@ $k$  for query  $q$ . So  $\text{Precision}(k)$  is the average of all Precision@ $k$  values over the set of queries, and likewise with  $\text{Recall}(k)$ .

*3.1.2. Mean average precision (MAP):* First we define at query node  $q$  the quantity

$$\text{AvP}(q) = \frac{1}{L} \sum_{k=1}^{N-1} P_q(k) r_q(k) \quad (7)$$

at each node, where  $N - 1$  is the number of nodes excluding the query node itself,  $L$  is the number of retrieved relevant

items and  $r_i(k)$  is an indicator taking value 1 if the item at rank  $k$  is a relevant item (actual neighbor) or zero otherwise (non-neighbor). Averaging further over query nodes, we obtain  $MAP = \frac{1}{|Q|} \sum_q AvP(q)$ .

In the remainder of this section, we explore these important issues:

- How should  $Q$  be sampled from  $V$ ? A related question is, how to present precision, recall, MAP, etc., with  $Q$  suitably disaggregated to understand how different LP algorithms behave on different nodes  $q \in Q$ ? (See Section 3.2.)
- Many graphs do not have link timestamps. For these, once  $Q$  is set, how should we sample edges incident on  $Q$  for training and testing? (See Section 3.3.)

### 3.2. Query node sampling protocols

In principle, the ranking prowess of an LP algorithm should be evaluated at *every* node. E.g., Facebook may recommend friends to all users, and there is potential satisfaction and payoff from every user. In practice, such exhaustive evaluation is intractable. Therefore, nodes are sampled; usually  $|Q| \ll N$ . On what basis should query nodes be sampled? In the absence of the social network counterpart to a commercial search engine’s query log, there is no single or simple answer to this question. LP algorithms often target predicting links that close triangles if/when they appear. 92% of all edges created on Facebook Iceland close a path of length two, i.e., a triangle [2]. These nodes are sampled as query nodes  $Q$ .

Besides providing comparison of overall performance averaged over query nodes, in order to gain insight into the dynamics of different LP algorithms, we need to probe deeper in the structure of the network and check the strength/weakness of the algorithm vis-a-vis various structures. In our work, we bucket the selected query nodes based on

- the number of neighbors,
- the number of triangles on which they are incident.

### 3.3. Edge sampling protocol

If edges in the input graph have creation timestamps, we can present a snapshot to the LP algorithm and simulate further passage of time to accrue its rewards. Even this happier situation raises many troublesome questions, such as when the snapshot is taken, the horizon for collecting rewards, etc., apart from (the composition of) the query node sample.

To complicate matters further, many popular data sets (some used in Section 5) do not have edge timestamps. One extreme way to dodge this problem is the leave-one-out protocol: remove exactly one edge at a time, train the LP algorithm, and make it score that edge. But this is prohibitively expensive.

Rather than directly sample edges, we first sample query nodes  $Q$  as mentioned in Section 3.2. This narrows our attention to  $|Q|(N-1)$  potential edge slots incident on query nodes. Fix query  $q$ . In the fully-disclosed graph,  $V \setminus q$  is partitioned into “good” neighbors  $G(q)$  and “bad” non-neighbors  $B(q)$ . We set a train sampling fraction  $\sigma \in (0, 1)$ . We sample  $\lceil \sigma |G(q)| \rceil$  good and  $\lceil \sigma |B(q)| \rceil$  bad nodes and present the

resulting *training* graph to the LP algorithm. ( $\sigma$  is typically 0.8 to 0.9, to avoid modifying the density and connectivity of the graph drastically and misleading LP algorithms.)

The good and bad training samples are now used to build our models as described in Section 4. The training graph, with the testing good neighbors removed, is used for co-clustering. This prevents information leakage from the training set. The remaining good neighbors and bad non-neighbors are used for testing. In case  $|G(q)| = \lceil \sigma |G(q)| \rceil$  or  $|B(q)| = \lceil \sigma |B(q)| \rceil$ , we discard  $q$ , introducing a small bias after our sampling of  $Q$ . Effectively this is a “sufficient degree” bias, which is also found in prior art [2, Section 4:  $K, \Delta$ ].

## 4. PROPOSED FRAMEWORK: CCLL

We have reviewed in Section 2 several LP approaches. Some (AA, RA, CRW) involve no learning, others [8] propose generative probabilistic models that best “explain” the current graph snapshot (and then the model parameters of the “explanation” can be used to predict future links, although they did not study this application). In recent years, direct prediction of hidden variables through conditional probability [13] or discriminative [23] models have proved generally superior to modeling the joint distribution of observed and hidden variables [24]. As we shall see in Section 5, this is confirmed even among our comparisons of prior work, where supervised random walk [2] is superior to unsupervised approaches. However before explaining our scheme we clearly define the *link prediction* problem.

### 4.1. Problem definition

We are given a snapshot of a social network, represented as a graph  $(V, E)$  with  $|V| = N$  and  $|E| = M$ . Let  $u \in V$  be a node (say representing a person). Edges may represent “friendship”, as in Facebook. Depending on the application or algorithm, the graph may be directed or undirected. The goal of LP is to recommend new friends to  $u$ , specifically, to rank all other nodes  $v \in V \setminus u$  in order of likely friendship preference for  $u$ . One ranking device is to associate a *score* with each  $v$ , and sort them by decreasing score. LP algorithms vary in how they assign this score. We can also think about LP as associating a binary hidden variable with the potential edge  $(u, v)$ , then estimating the probability that this variable has value 1 (or true), based on observations about the currently revealed graph. The LP algorithm is considered high quality if the user accepts many proposed friends near the top of the ranked list. In case of large  $V$ , LP systems often restrict the potential set of  $vs$  to ones that have a common neighbor  $c$ , i.e.,  $(u, c)$  and  $(c, v)$  already exist in  $E$ .

### 4.2. Overview of two-level discriminative framework

LP can also be regarded as a classification problem: given a pair of nodes  $u, v$ , we have two class labels (“link” vs. “no link”) and the task is to predict the correct label. To estimate a confidence in the (non) existence of a link, we will aggregate several kinds of input signals, described throughout the rest of this section. Apart from subsuming existing signals from

one or more of AA, RA, and CRW, we will harness two new signals. First, in Section 4.3, we will describe a local learning process to determine effective similarity between two given nodes. Unlike AA and other node-pair signals, our new approach recognizes that propensity of linkage is not purely a function of node similarity; it changes with neighborhood. Second, in Section 4.4 we describe how to harness the output of a co-clustering of the graph’s adjacency matrix to derive yet more features. To our knowledge coclustering has never been used in this manner for LP.

For each proposed node pair  $u, v$ , these signals will be packed as features into a feature vector  $f(u, v) \in \mathbb{R}^d$  for some suitable number of features  $d$ . We estimate a *global model*  $\nu \in \mathbb{R}^d$ , such that the confidence in the existence of edge  $(u, v)$  is directly related to  $\nu \cdot f(u, v)$ .  $f(u, v)$  will consist of several blocks or sub-vectors, each with one or more elements.

- $f(u, v)[AA]$  is the block derived from the Adamic-Adar (AA) score (1). (We can also include other local scores in this block.)
- $f(u, v)[LL]$  is the block derived from local similarity learning (Section 4.3).
- $f(u, v)[CC]$  is the block derived from co-clustering (Section 4.4).

As we shall demonstrate in Section 5, these signals exploit different and complementary properties of the network. If  $y(u, v) \in \{0, 1\}$  is the observed status of a training edge, we can find the weights ( $\nu$ ) using a SVM and its possible variations. The details will be discussed in Section 4.5.

To exploit possible interaction between features, we can construct suitable kernels [3]. Given we have very few features, a quadratic (polynomial) kernel can be implemented by explicitly including all quadratic terms. I.e., we construct a new feature vector whose elements are

- $f(u, v)[i]$  for all indices  $i$ , and
- $f(u, v)[i] f(u, v)[j]$  (ordinary scalar product) for all index pairs  $i, j$ .

We can also choose an arbitrary informative subset of these. We will now describe the three blocks of features.

### 4.3. Learning local similarity

An *absolute* notion of similarity between  $u$  and  $v$ , based on node features  $\theta_u, \theta_v$ , is not strongly predictive of linkage; it also depends on the typical *distribution* of similarity values in the neighborhood [5]. Also, the presence or absence of edge  $(u, v)$  rarely determined by nodes far from  $u$  and  $v$ . Keeping these in mind, the first step of the algorithm learns the typical (dis)similarity between  $u$  and  $v$  and their common neighbors. We term this the *reference* dissimilarity. We then use this to predict the chance of link  $(u, v)$  arriving.

Let  $\Gamma(u)$  be the (immediate) neighbors of  $u$ . We will model the *edge dissimilarity* between  $u$  and  $v$  as

$$\Delta_w(u, v) = w_{uv} \cdot |\theta_u - \theta_v|, \quad (8)$$

where  $\theta_u$  is a node feature vector associated with  $u$ , and  $|\dots|$  denotes the *elementwise* absolute value of a vector, e.g.,

$|(-2, 3)| = (2, 3)$ , although other general combinations of  $\theta_u$  and  $\theta_v$  are also possible [2].  $w_{uv}$  is the weight vector fitted *locally* for  $u, v$ . (Contrast this with the global  $\nu$  above, and the final proposal in SRW [2] that fits a single model over all node pairs.)

**4.3.1. Finding  $w_{uv}$  and reference dissimilarity:** Throughout this work, and consistent with much LP work, we assume that edges are associative or unipolar, i.e., there are no “dislike” or antagonistic links. Similar to AA and friends, when discussing node pair  $u, v$ , we restrict our discussion to the vicinity  $N = \Gamma(u) \cup \Gamma(v)$ .

For  $A \subseteq V \setminus u, A \neq \emptyset$ , we extend definition (8) to the *set dissimilarity*

$$\Delta_w(u, A) = \frac{1}{|A|} \sum_{v \in A} \Delta_w(u, v). \quad (9)$$

We define  $\Delta_w(u, \emptyset) = 0$ .  $\Delta_w(u, A)$  is the average dissimilarity between  $u$  and  $A$ . Note that  $\Delta_w(u, \{v\})$  is simply  $\Delta_w(u, v)$ .

The key idea here is that, if there is an edge  $(u, v)$ , we want to choose  $w_{u,v}$  such that  $\Delta_w(u, v)$  is low, *relative to* node pairs that are not neighbors. Conversely, if  $(u, v)$  is not an edge, we want the dissimilarity to be large relative to nearby node pairs that are neighbors. We codify this through the following four constraints:

$$\begin{aligned} \Delta_w(u, \Gamma(u) \setminus \Gamma(v)) &\leq \alpha \Delta_w(u, v) \\ \Delta_w(v, \Gamma(v) \setminus \Gamma(u)) &\leq \alpha \Delta_w(u, v) \\ \Delta_w(u, \Gamma(v) \setminus \Gamma(u)) &\geq \beta \Delta_w(u, v) \\ \Delta_w(v, \Gamma(u) \setminus \Gamma(v)) &\geq \beta \Delta_w(u, v) \end{aligned} \quad (10)$$

Figure 1 illustrates the constraints. Here  $\alpha, \beta$  are suitable multiplicative margin parameters. Smaller (larger) value of  $\alpha$  ( $\beta$ ) allows a lower (higher) dissimilarity between the connected (disconnected) nodes. Here, we have experimentally selected  $\alpha$  and  $\beta$ .

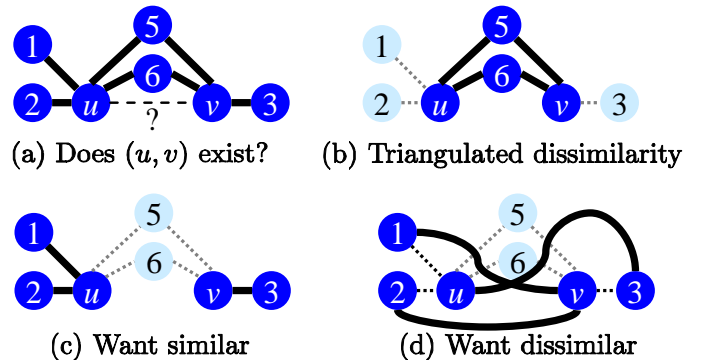


Figure 1. Local dissimilarity constraints.

Subject to the above constraints (10), we wish to choose  $w$  so as to minimize  $\Delta_w(u, v)$ . This is a standard linear program, which, given the typically modest size of  $\Gamma(u) \cup \Gamma(v)$ , runs quite fast.

4.3.2. *Computation of LL features:* The linear program outputs  $w_{uv}^*$ , from which we can compute

$$\delta_{uv} = w_{uv}^* \cdot |\theta_u - \theta_v|. \quad (11)$$

But is  $\delta_{uv}$  larger than “expected”, or smaller? Plugging in the raw value of  $\delta_{uv}$  into our outer classifier may make it difficult to learn a consistent model  $\nu$  globally across the graph. Therefore, we also compute the *triangulated dissimilarity* between  $u$  and  $v$ , using common neighbors  $i$ , as

$$\begin{aligned} \bar{\Delta}_{w^*}(u, v) &= \sum_{i \in \Gamma(u) \cap \Gamma(v)} \frac{\Delta_{w^*}(i, u) + \Delta_{w^*}(i, v)}{|\Gamma(u) \cap \Gamma(v)|} \\ &= \Delta_{w^*}(u, \Gamma(u) \cap \Gamma(v)) + \Delta_{w^*}(v, \Gamma(u) \cap \Gamma(v)). \end{aligned} \quad (12)$$

Finally, we return

$$f(u, v)[LL] = \bar{\Delta}_{w^*}(u, v) - \delta_{uv}. \quad (13)$$

If  $f(u, v)[LL]$  is large and positive, it expresses confidence that link  $(u, v)$  will appear; if it is large and negative, it expresses confidence that it will not. Around zero, the LL feature is non-committal; other features may then come to the rescue.

#### 4.4. Co-clustering and “surprise”

Given a dyadic relation represented as a matrix, co-clustering [6] partitions rows and columns into row groups and column groups. We can think of the rows and columns of the input matrix being reordered so that groups are contiguous. The intersection of a row group and column group is called a *block*. The goal of co-clustering is to choose groups so that the blocks are *homogeneous*, i.e., edges within a block appear uniformly dense, with no finer structure (stripes) based on rows or columns. Co-clustering uses a data compression formalism to determine the optimal grouping.

Consider a query node pair  $u, v$  where we are trying to predict whether edge  $(u, v)$  exists. E.g.,  $u$  may be a person,  $v$  may be a movie, and we want to predict if  $u$  will enjoy watching  $v$ . In this person-likes-movie matrix, as a specific example, there may be row groups representing clusters of people that like most movies, and there may be column groups representing clusters of classic movies that most people like. In general, the block in which the matrix element  $[u, v]$  is embedded, and in particular, its edge density  $d(u, v)$ , gives a strong prior belief about the existence (or otherwise) of edge  $(u, v)$ , and could be the feature  $f(u, v)[CC]$  in and of itself.

Although block density  $d(u, v) \in [0, 1]$ , the penalty for deviating from it in the ultimate link decision is not symmetric (thanks again to graph sparsity). So a better formalism to capture a coclustering-based feature is the “surprise value” of an edge decision for node pair  $u, v$ . As an extreme case, if a non-edge (value 0) is present in a co-cluster block where all remaining elements are 1 (edges), it causes large surprise. The same is the case in the opposite direction.

There are various ways of expressing this quantitatively. One way of expressing it is that if an edge  $(u, v)$  is claimed to exist, and belongs to a block with an edge density  $d(u, v)$ , the

surprise is inversely related to  $d(u, v)$ ; in information theoretic terms, the surprise is  $-\log d(u, v)$  bits. (So if  $d(u, v) \rightarrow 0$ , yet the edge exists, the surprise goes to  $+\infty$ .) Similarly, if the edge does not exist, the surprise is to  $-\log(1 - d(u, v))$  bits.

#### 4.5. The discriminative learner for global model $\nu$

In order to obtain the best LP accuracy, the above signals need to be combined suitably. For each edge, there are two classes (present/absent). One possibility is to label these  $+1, -1$ , and fit the predictor  $\hat{y}_{uv} = \text{sign}(\nu \cdot f(u, v))$ .

4.5.1. *Loss function:*  $\nu$  can be learnt to minimize various loss functions. The simplest is 0/1 edge misclassification<sup>3</sup> loss  $\sum_{q \in Q} \frac{1}{N-1} \sum_{v \neq q} \mathbb{I}[\hat{y}_{qv} \neq y_{qv}]$ , which is usually replaced by a convex upper bound, the hinge loss

$$\sum_{q \in Q} \frac{1}{|G(q) \cup B(q)|} \sum_{b \in G(q) \cup B(q)} \max\{0, y_{qb} \nu \cdot f(u, v) - 1\}. \quad (14)$$

As we have discussed in Section 3.1, for ranking losses, it is better to optimize the AUC, which is closely related [11] to the pairwise loss

$$\sum_{q \in Q} \frac{1}{|G(q)| |B(q)|} \sum_{g \in G(q), b \in B(q)} \mathbb{I}[\nu \cdot f(q, b) \geq \nu \cdot f(q, g)], \quad (15)$$

which is again usually approximated by the hinge loss

$$\sum_{q \in Q} \frac{1}{|G(q)| |B(q)|} \sum_{g \in G(q), b \in B(q)} \max\{0, 1 - \nu \cdot (f(q, g) - f(q, b))\} \quad (16)$$

Joachims [11] offers to directly optimize  $\Lambda$  for several ranking objectives; we choose area under the ROC curve (AUC) for training  $\Lambda$ , although we evaluate the resulting predictions using MAP. During inference, given  $q$ , we find  $\nu \cdot f(q, v)$  for all  $v \neq q$  and sort them by decreasing score.

4.5.2. *Feature map:* We now finish up the design of  $f(u, v)[AA], f(u, v)[LL]$  and  $f(u, v)[CC]$ . The first two are straight-forward, we simply use the single scalar (1) for  $f(u, v)[AA]$ , and  $f(u, v)[LL]$  is also a single scalar as defined in (13). The  $f(u, v)[CC]$  case is slightly more involved, and has two scalar elements, one for each surprise value:

- $-\log d(u, v)$  for the “link exists” case, and
- $-\log(1 - d(u, v))$  for the “edge does not exist” case.

Accordingly,  $\nu$  will have two model weights for the CC block, and these will be used to balance the surprise values from training data. The soundness of the above scheme follows from structured learning feature map conventions [11], [23]. We defer the elementary algebraic details to the full version of this paper. Thus,  $f(u, v)$  has a total of four elements.

## 5. EXPERIMENTS

We compare CCLL against several strong baselines such as Adamic-Adar (AA) [1], RA [19], Cumulative Random Walk (CRW) [19], Supervised Random Walk (SRW) [2], and Generative Model (GM) [8]. RA computes the score in a similar manner like AA, and therefore gives almost same performance. Therefore, we omit RA and only present those

<sup>3</sup> $\mathbb{I}[B]$  is 1 if  $B$  is true, 0 otherwise.

Dataset	N	E	$n(a)$	$d_{avg}$
Movielens	3952	5669	18	2.8689
CiteSeer	3312	4732	3703	2.7391
Cora	2708	5429	1433	3.89
WebKb	877	1608	1703	2.45
NetFlix	17770	20466	64	2.3034

Figure 2. Summary of the datasets, where  $N$  is the number of items,  $E$  is the total number of links,  $n(a)$  is the number of features and  $d_{avg}$  is the average degree.

for AA. Apart from using LL as features to CCLL, we run LL independently as a baseline.

### 5.1. Datasets used

We used the following popular public data sets, also summarized in Figure 2.

**Movielens [26]:** It has 6040 users and 3952 movies. Each user has rated at least one movie. Each movie has features which are a subset of a set of 18 nominal attributes (e.g. animation, drama etc.). From the raw data we constructed a “social network” between movies where two movies have an edge if they have at least a certain number of common viewers. By choosing the minimum number of common viewers to be 100, we obtain a network with 3952 nodes and 5669 edges.

**CiteSeer [25]:** The CiteSeer dataset consists of 3312 scientific publications and the citation network consists of 4732 links. Each publication is tagged with a set of keywords. Total number of keywords is 3703.

**Cora [25]:** The Cora dataset consists of 2708 scientific publications and the citation network consists of 5429 links. Here the total number of keywords is 1433.

**WebKb [25]:** The WebKb dataset consists of 877 scientific publications and the citation network consists of 1608 links. Here the total number of keywords is 1703.

**Netflix [9]:** The Netflix dataset consists of 2649429 users and 17770 movies. Each user has rated at least one movie. Each movie has 64 features obtained by SVD from many factors. From the raw data we constructed a “social network” of movies where two movies have an edge if they have at least a certain number of common viewers. By choosing the minimum number of common viewers to be 20, we obtain a network with 17770 nodes and 20466 edges.

### 5.2. Performance of CCLL compared to other algorithms

Figure 4 gives a comparative analysis of MAP (Mean Average Precision) values for all datasets and algorithms, and Figure 3 gives a more detailed view of precision vs. recall. We observe that, for all datasets, the overall performance of CCLL is substantially better than all other methods.

Performance of the probabilistic generative model is particularly poor. This was surprising to us, given stochastic

Dataset	CCLL	LL	AA	CRW	GM	SRW
Netflix	0.6017	0.4750	0.5381	0.5428	0.1268	0.4564
Movielens	0.8747	0.8133	0.5341	0.5784	0.20	0.8114
CiteSeer	0.7719	0.7393	0.6649	0.5309	0.1452	0.6281
Cora	0.7234	0.6805	0.6135	0.4726	0.0583	0.6274
WebKb	0.8583	0.7505	0.6035	0.5736	0.3360	0.6693

Figure 4. Mean average precision over all algorithms and datasets.

block models (SBMs) seem ideally suited for use in LP. Closer scrutiny showed model sparsity as a likely culprit, at least in case of Ho *et al.*’s formulation. They derive a tree-structured hierarchical clustering of the social network nodes, where the number of hierarchy nodes is much smaller than  $N$ , the number of social network nodes. Their model assigns a score to an edge  $(u, v)$  that depends on the hierarchy paths to which  $u$  and  $v$  are assigned. Since the number of hierarchy nodes is usually much smaller than the number of social nodes, the score of neighbors of any nodes have a lot of ties, which reduces ranking resolution. Therefore, MAP suffers. In contrast, the coarse information from co-clustering (CC) is only a feature into our top-level ranker.

AA, RA, CRW all produce comparable performance. All these methods solely depend on link characteristics, for example AA and RA depending on the number of triangles a node is part of, hence they miss out the important node or edge feature information. Regarding CRW, as  $t$  goes to  $\infty$ , it doesn’t converge, and there is no consistent global  $t$  for best MAP. SRW, which performs best among the baselines, uses node and link features (PageRank) but not community based (co-clustering) signal. Moreover, SRW learns only one global weight vector, unlike  $w_{uv}$  in LL, a signal readily picked up by CCLL. We also found the inherent non-convexity of SRW to produce suboptimal optimizations. LL is next to SRW in all data sets except NetFlix. This is because the number of features in Netflix is small and the values assumed by each feature is very diverse, making the feature-based local prediction strategy ineffective.

A possible explanation of the superior performance of CCLL can be that the underlying predictive modules (LL, AA, CC) perform well in complementary zones which CCLL can aggregate effectively. In order to probe into this aspect we make a detailed study of the performance of the various algorithms with respect to various distribution of work load (elaborated in Section 5.6).

### 5.3. Stability to Sampling

Among all methods, CCLL and SRW use machine learning. Hence in order to train the model, we randomly select a certain fraction of edges (say  $TS\%$ ) and the same fraction of non-edges from the network. CRW is an unsupervised algorithm but since it performs a global random walk it is affected by the sampling, the performance deteriorating when many edges are removed. Figure 5 shows the variation of performance with training sets of different sizes. We conducted the experiment with 80% and 90% training samples. When we decrease the

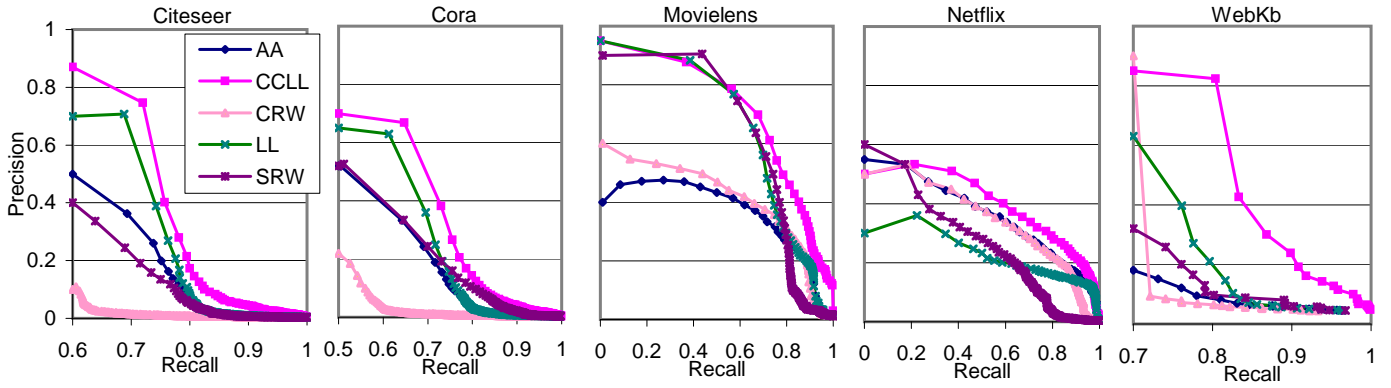


Figure 3. Precision vs. recall curves for all data sets and algorithms.

Dataset	TS (%)	CCLL	CRW	SRW
Netflix	80	0.5263	0.4493	0.3849
	90	0.6017	0.5428	0.5567
Movielens	80	0.8672	0.5018	0.7789
	90	0.8740	0.5784	0.8114
Citeseer	80	0.7000	0.3295	0.5567
	90	0.7719	0.5309	0.6281
Cora	80	0.6803	0.3400	0.5516
	90	0.7203	0.4726	0.6274
WebKb	80	0.8309	0.3360	0.5931
	90	0.8583	0.5736	0.6693

Figure 5. Variation of accuracy with different training set sizes.

sample size from 90% to 80%, the performance deteriorates for all methods. But the deterioration is much smaller in CCLL compared to CRW and SRW. This is because CCLL picks up strong signals from the AA and LL features. AA and LL work solely on local factors. Deletion of an additional 10% of edges hardly affects AA or LL score.

#### 5.4. Importance of various features

Figure 6 dissects the various features involved in CCLL, fixing at 90% sampling rate henceforth. To understand the role of different features (local link structure, global community structure), we build our SVM model eliminating either LL or CC and calculate the ranking accuracy (MAP). The results show that the absence of each of the signals (LL and CC) significantly deteriorates the performance. However, closer scrutiny showed the interesting property that the deterioration occurs in different zones, that is, it is almost always true that the node whose MAP gets affected by elimination of LL does not face such problem when CC is removed.

#### 5.5. Effect of quadratic terms

The results presented so far used only linear features. Figure 7 shows the results obtained with quadratic features (Section 4.1), compared to linear features (90% sample). The data sets are arranged in decreasing order of size. I.e., Netflix has the largest number of nodes and WebKb the smallest. It is seen that for larger data set the inclusion of quadratic terms

Dataset	CCLL	$SVM(LL, AA)$	$SVM(LL, CC)$
Netflix	0.6017	0.5761	0.5478
Movielens	0.8740	0.8436	0.8483
Citeseer	0.7719	0.7467	0.7677
Cora	0.7203	0.7044	0.7139
WebKb	0.8583	0.8106	0.8470

Figure 6. Feature ablation study.

Dataset	CCLL	LL+AA+CC	Improvement Factor
Netflix	0.6017	0.5755	1.045
Movielens	0.8740	0.8565	1.020
Citeseer	0.7719	0.7677	1.006
Cora	0.7203	0.7220	0.997
WebKb	0.8583	0.8524	1.006

Figure 7. Effect of including quadratic features.

boosts accuracy. The enhancement of performance indicates the role played by possible interaction of the features. In other words, we can conclude that not only local link structure, attributes and community level signals have important roles here, but also they interact or affect each other which also play a crucial role in link prediction. The interaction can be exploited better in a more complex model if there is more training data.

#### 5.6. Workload Distribution

In this section, we present some comparative analysis between CCLL and other four best benchmark algorithms on two representative datasets: Netflix and Movielens (Figures 8 and 9). The choice is motivated by the fact that Movielens gives best performance and Netflix gives worst performance (with CCLL) among all the five datasets. Netflix has few features while Movielens is feature-rich. Query nodes are bucketed based on

- the number of neighbors they have (changes from sparse to dense), and
- the number of triangles formed.

Each bucket holds roughly one-sixth of the nodes.



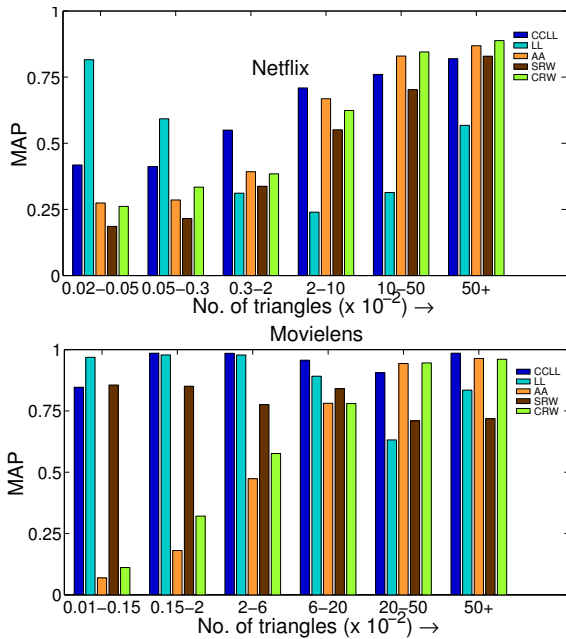


Figure 8. Workload distribution based on number of triangles.

The workload distribution highlights the nature of each algorithm. The behavior of the algorithms is similar for the two workload distributions. It is seen that AA and CRW which solely depend on link structure improve as the graph becomes more dense (number of neighbor increases) or become more social (number of triangle increases). The two feature based algorithms, LL and SRW, perform well in the sparse zone, and the improvement in the dense (more social) zone is observed but not as significant as the two link-based algorithms. Clearly, in these two zones (sparse and dense), two different classes of algorithm work well.

CCLL performs well in all the zones by appropriately learning signals in each zone. However, it even improves upon its two constituents in each and every zone. From Figure 9 we observe that CCLL performs best (substantially better than LL and AA), at intermediate density. There are two reasons behind it. Even though the graph is sparse, in these regions,  $|G(q)|$  and  $|B(q)|$  are not far apart, which helps CCLL to train better. Second, nodes in these zones are member of community coclustering structures with informative block densities and surprise feature. Factoring in the community signal helps to positively interpret the surprise.

### 5.7. Variation of performance across different data sets

From Figure 4 we observe the wide variation of MAP over various datasets, across all algorithms. The variation may be due to various graph properties like density, clustering coefficient or due to the (un)structureness of the constituent features. We organize the results of MAP with respect to the above mentioned three parameters and present the same through Figure 10. Following the first sub-figure, we see Movielens is having the most well-structured feature space. It consists of genre and it is usually observed that people

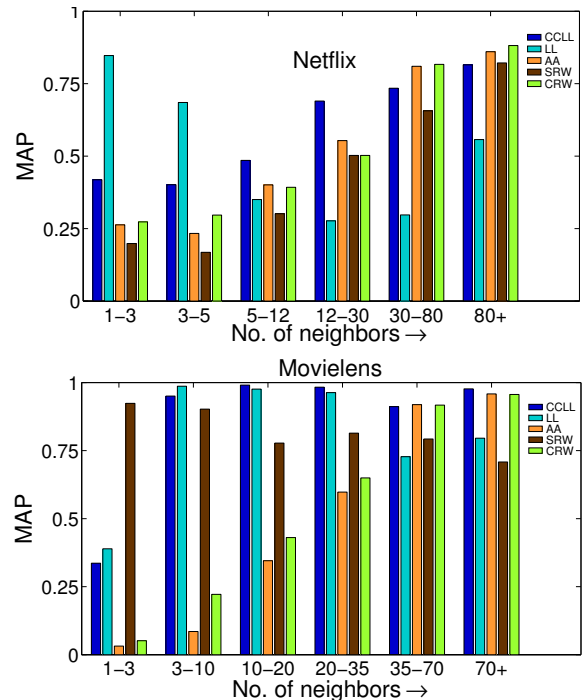


Figure 9. Workload distribution based on number of neighbors.

usually like similar movies. We find that it has the highest MAP. Feature richness is not a perfect predictor of high MAP. Netflix has rich features but perform relatively poorly. Like MovieLens, Netflix is also a movie-movie network. But its features are not as informative, because they are derived from many other factors (like year of the movie, actors, director etc.) apart from genre, and the distillation process seems noisy.

The other predictor of MAP is the average density (subfigure (b)), higher density means more signal to the classifier. Hence, MAP normally increases with increasing density, that explains Netflix which has very low average degree perform poorly. The third factor which enhances accuracy is local connectedness which is captured through clustering coefficient and is plotted in subfigure (c). The three paper repositories, WebKb, Cora and Citeseer, have very unstructured feature space (words) as the features are polluted by polysemy, synonymy, etc. However, the high clustering coefficient of WebKb balances this disadvantage and is a key reason for its good performance. For the other algorithms LL and SRW, the same ranking is maintained, although the performance gap between Movielens (first) and WebKb (second) increases. This is in line with the same observation mentioned before that LL and SRW cannot exploit link structure well. The ranking in CRW and AA are different and more in line with the ranking of the dataset with respect to density and clustering coefficient.

## 6. CONCLUSION

We described a new two-level learning algorithm for link prediction. At the lower level, we learn a local similarity model across edges. At the upper level, we combine this

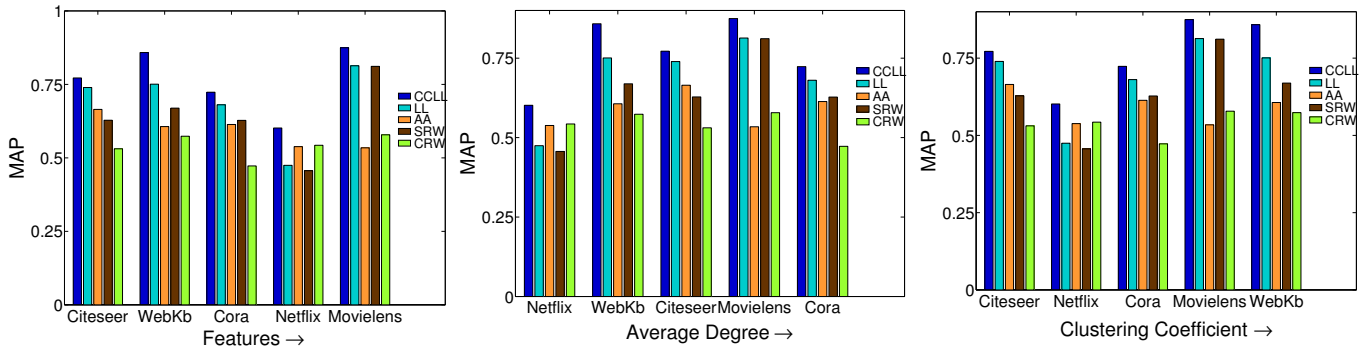


Figure 10. Variation of MAP over various datasets w.r.t. feature richness, average degree and clustering coefficient. (The same data is presented in three different orders.)

with co-clustering signals using a SVM. On diverse standard public data sets, the resulting link predictor outperforms recent LP algorithms. Another contribution of this paper is to systematically understand the areas of inefficiency of recent LP algorithms and consequently establish the importance of this two-level learning scheme, and the key features we use. We show that our algorithm consistently outperforms four strong baselines when link information is neither too sparse nor too dense. In practice, a large amount of requests for link recommendation will actually come from this zone, hence the significance of the result can be even more than what is stated in the paper. In future work, it will be of interest to combine the signals we exploit with supervised personalized PageRank [2]. Another possibility is to replace item-wise or pairwise losses with list-wise losses suitably aggregated over query samples.

**Acknowledgement:** This work was supported by Google India under the Google India PhD Fellowship Award.

#### REFERENCES

[1] L. A. Adamic and E. Adar. Friends and neighbors on the Web. *Social Networks*, 25(3):211 – 230, 2003.

[2] L. Backstrom and J. Leskovec. Supervised random walks: predicting and recommending links in social networks. In *WSDM Conference*, pages 635–644, Hong Kong, 2011.

[3] C. M. Bishop. *Pattern Recognition and Machine Learning*. Springer, 2006.

[4] D. Chakrabarti, S. Papadimitriou, D. S. Modha, and C. Faloutsos. Fully automatic cross-associations. In *SIGKDD Conference*, pages 79–88, Seattle, WA, USA, 2004. ACM.

[5] A. De, M. S. Desarkar, N. Ganguly, and P. Mitra. Local learning of item dissimilarity using content and link structure. In *Proceedings of the sixth ACM conference on Recommender systems, RecSys '12*, pages 221–224, 2012.

[6] I. S. Dhillon, S. Mallela, and D. S. Modha. Information-theoretic co-clustering. pages 89–98, Washington, D.C., 2003. ACM.

[7] P. Doyle and L. Snell. Random walk and electric networks. In *Mathematical Association of America*, 1984.

[8] Q. Ho, J. Eisenstein, and E. P. Xing. Document hierarchies from text and links. In *WWW Conference*, pages 739–748, Lyon, France, 2012. ACM.

[9] <http://www.netflixprize.com>.

[10] G. Jeh and J. Widom. Scaling personalized web search. In *WWW Conference*, pages 271–279, 2003.

[11] T. Joachims. A support vector method for multivariate performance measures. In *ICML*, pages 377–384, 2005.

[12] L. Katz. A new status index derived from sociometric analysis. *Psychometrika*, 18(1):39–43, Mar. 1953.

[13] J. Lafferty, A. McCallum, and F. Pereira. Conditional random fields: Probabilistic models for segmenting and labeling sequence data. In *ICML*, pages 282–289, 2001.

[14] A. N. Langville and C. D. Meyer. Deeper inside PageRank. *Internet Mathematics*, 1(3):335–380, 2004.

[15] D. D. Lee and H. S. Seung. Algorithms for non-negative matrix factorization. In *NIPS Conference*, 2001.

[16] D. Liben-Nowell and J. Kleinberg. The link-prediction problem for social networks. *Journal of the American Society for Information Science and Technology*, 58(7):1019–1031, 2007.

[17] R. N. Lichtenwalter, J. T. Lussier, and N. V. Chawla. New perspectives and methods in link prediction. In *SIGKDD Conference*, pages 243–252, Washington, DC, USA, 2010. ACM.

[18] T.-Y. Liu. Learning to rank for information retrieval. In *Foundations and Trends in Information Retrieval*, volume 3, pages 225–331. Now Publishers, 2009.

[19] L. Lu and T. Zhou. Link prediction in complex networks: A survey. *Physica A: Statistical Mechanics and its Applications*, 390:1150–1170, Mar. 2011.

[20] P. Sarkar, D. Chakrabarti, and A. W. Moore. Theoretical justification of popular link prediction heuristics. In *IJCAI*, pages 2722–2727, Barcelona, Spain, 2011. AAAI Press.

[21] H. Tong, C. Faloutsos, and Y. Koren. Fast direction-aware proximity for graph mining. In *SIGKDD Conference*, pages 747–756. ACM, 2007.

[22] H. Tong, C. Faloutsos, and J.-Y. Pan. Fast random walk with restart and its applications. In *ICDM*, 2006.

[23] I. Tschantzaris, T. Joachims, T. Hofmann, and Y. Altun. Large margin methods for structured and interdependent output variables. *JMLR*, 6(Sep):1453–1484, 2005.

[24] V. Vapnik. *Statistical Learning Theory*. Wiley, Chichester, 1998.

[25] [www.cs.umd.edu/projects/linqs/projects/lbc](http://www.cs.umd.edu/projects/linqs/projects/lbc).

[26] [www.grouplens.org](http://www.grouplens.org).